Wave overtopping and toe scouring at a plain vertical seawall with shingle foreshore:

A Physical model study

M. Salauddin[1*] and J. M. Pearson[1]

[1]School of Engineering, University of Warwick, Coventry, CV47AL, UK

Abstract

This paper describes a physical model study to investigate the wave overtopping and toe scouring at a plain vertical wall with a shingle foreshore. A matrix of 180 experimental test conditions were performed in a 2D wave flume, with an approximate scale of 1:50. The study investigates the baseline overtopping characteristics at a plain vertical wall on an impermeable 1:20 foreshore slope and compares the results with two permeable 1:20 shingle beach foreshores with prototype d_{50} values of 13 mm, and 24 mm respectively. For impulsive wave conditions, it was found that the mean overtopping rate was reduced by factor 3 for the d_{50} of 13 mm, and a factor of 4 for the d_{50} of 24 mm. For non-impulsive waves, the reduction factors were 1.5 for d_{50} of 13 mm and 2 for d_{50} of 24 mm. Prior to this study, limited design guidance was available to predict the mean overtopping discharges and mean sediment rates at vertical seawalls on permeable shingle foreshores. Therefore, a new set of prediction formulae are proposed in this study, based on the new laboratory test results, and a comparison with the available prediction methods in literature for vertical seawalls subjected to both impulsive and non-impulsive wave conditions.

*Corresponding Author

E-mail address: m.salauddin@warwick.ac.uk (M. Salauddin)

Keywords

Overtopping, Scouring, Shingle foreshore, Impermeable foreshore, Vertical seawalls, Sediment discharge.

1. Introduction

Shingle or gravel beaches and barriers are an effective approach of natural coastal defence ‘with high ecological, amenity and aesthetic value’ (Obhrai et al., 2008). Nevertheless, coastal hazards such as impairment of coastal infrastructure and coastal flooding can occur at shingle beaches and barriers due to wave overtopping, over-washing, erosion and barrier breaching processes (EurOtop, 2016; McCall et al., 2015). Beach material contained within the overtopping waves can be particularly hazardous to personnel.

The performance of the coastal structures such as vertical or near vertical seawalls and harbour breakwaters can be classified in many ways, usually using complex functions of wave and geometric parameters. For example, many man-made coastal structures are designed to limit overtopping, in which predictions are derived from general empirical formulae fitted to laboratory measurements. Whilst these structures may be efficient in the mitigation of wave overtopping, they may be subject to impulsive wave breaking giving sudden and violent overtopping flows and scouring at toe, the interactions of which are currently difficult to describe with any degree of certainty.

This research was focussed to improve the physical understanding and description of the key coastal processes along the wave / structure interface specifically to characterise the overtopping and toe scouring at vertical walls with a permeable shingle beach foreshore. These key coastal processes at coastal structures on an impermeable foreshore configuration have been widely described by many researchers over the years, see EurOtop (2016). However, little knowledge is available on the performance of these processes at vertical structures with permeable shingle beach foreshores. This study presents the baseline overtopping and scouring characteristics at a plain vertical wall on an impermeable 1:20 foreshore slope, and compares the results with existing empirical predictions (EurOtop, 2016). These results are then compared two permeable 1:20 shingle beach foreshores with prototype d_{50} values of 13 mm, and 24 mm respectively.

2. Previous Studies

Over the years, although a number of investigations on coastal morphodynamics were carried out on sandy beaches, very few studies were undertaken on gravel beaches (De San Román-Blanco et al., 2006). To predict the cross-shore profile change for a gravel beach, there are some empirical models available in literature, such as empirical models prescribed by Lorang (2002); Van der Meer (1992); Van Hijum and Pilarczyk (1982). Apart from these, Gentile and Giasi 2003 described a methodological approach for the remodelling of shingle beaches which has been then applied for the evaluation of re-naturalization process of a gravel beach named Torre del Porto in the South-East of Italy, see Altomore and Gentile 2011, 2013. Besides empirical models, recent physical model studies have been undertaken to investigate the dynamic response of gravel barriers and beaches under the combined action of tides and waves and storm. For instance, a large-scale laboratory studies on gravel barriers and beaches have been undertaken in the BARDEX project, see details Williams et al. (2012a). Afterwards, the numerical simulations of gravel beaches using XBeach model were validated with the gathered laboratory datasets combined with field studies on gravel beaches, see McCall et al. (2015); Williams et al. (2012b).

A paucity of parametric studies has been devoted to the breaching, overtopping and overwash process of gravel beaches and barriers, see Bradbury (2000); Matias et al. (2012); Obhrai et al.

(2008); Pearson (2010). Based on the test results of 2D experimental investigations in a wave flume, Pearson (2010) reported that a reduction on the mean overtopping rate can be achieved with the use of a permeable shingle beach (mobile bed) compared to a fixed impermeable beach (solid bed).

2.1 Empirical predictions of overtopping

The existing empirical prediction formulae are mainly based on the laboratory measurements with the use of an impermeable foreshore slope in front of the structure. Recently, EurOtop (2016), an updated version of EurOtop (2007) overtopping manual was published with revised empirical equations to estimate mean overtopping discharge rates at plain vertical walls with and without foreshores. In general, in a relatively deep water, waves approaching structures are small compared to the local water depth and reflected back, usually without breaking, conditions termed ‘pulsating’ or ‘non-impulsive’. On the other hand, if the waves are large relative to the water depth, then they can break onto the structure, conditions termed ‘impulsive’, see Bruce et al. (2010); Pearson et al. (2002).

For this study, the measured mean overtopping rates are compared with overtopping predictions provided by the overtopping manual EurOtop (2016), see Equations 1 – 3 considering a foreshore slope in front of the vertical wall.

For non-impulsive conditions ($h_t^2/(H_{m0}L_{m-1,0}) > 0.23$),

$$\frac{q}{\sqrt{gH_{m0}^3}} = 0.05 \exp\left(-2.78\frac{R_c}{H_{m0}}\right) \tag{1}$$

For impulsive conditions ($h_t^2/(H_{m0}L_{m-1,0}) \leq 0.23$),

$$\frac{q}{\sqrt{gH_{m0}^3}} = 0.011\left(\frac{H_{mo}}{h_t s_{m-1,0}}\right)^{0.5} \exp\left(-2.2\frac{R_c}{H_{m0}}\right) \qquad \text{for } 0 < \frac{R_c}{H_{m0}} < 1.35 \tag{2}$$

and

$$\frac{q}{\sqrt{gH_{m0}^3}} = 0.0014\,(\frac{H_{mo}}{h_t s_{m-1,0}})^{0.5}\,(\frac{R_c}{H_{mo}})^{-3} \qquad \text{for } \frac{R_c}{H_{m0}} \geq 1.35 \tag{3}$$

where, H_{mo} is the spectral significant wave height, R_c is the crest freeboard of the structure, h_t is the water depth at the toe of the structure, g is the gravitational acceleration (=9.81 m/s^2), q is the mean overtopping discharge per meter structure width (m^3/s per m or l/s per m), $T_{m-1,0}$ is the spectral wave period calculated from statistical wave spectra analysis, $L_{m-1,0}$ is the deep water wave length based on spectral wave period $(=\frac{gT_{m-1,0}^2}{2\pi})$ and $s_{m-1,0}$ is the wave steepness based on spectral wave period $(=\frac{H_{m0}}{L_{m-1,0}})$.

For the estimation of maximum individual overtopping volume and proportion of overtopping waves, the empirical formuale provided by EurOtop (2016) are adopted in this work, see Equations 4-9. The maximum individual overtopping volume (V_{max}) at a plain vertical structure can be approximated by knowing the number of overtopped waves (N_{ow}) in a sequence for both non-impulsive and impulsive conditions, see Equation 4 (EurOtop, 2016).

Maximum individual overtopping volume (V_{max}),

$$V_{max} = a(\ln N_{ow})^{1/b} \tag{4}$$

where, V_{max} is the maximum overtopping volume per meter structure width (m^3 per m or l per m), N_{ow} is the number of overtopping waves, a is the Weibull scale factor and b is the Weibull shape factor.

For non-impulsive conditions, shape factor b

$$b = \begin{cases} 0.66 & \text{for } \mathrm{s}_{\mathrm{m-1,0}} = 0.02 \\ 0.88 & \text{for } \mathrm{s}_{\mathrm{m-1,0}} = 0.04 \end{cases} \qquad h_t^2/(H_{m0}L_{m-1,0}) > 0.23 \tag{5}$$

For impulsive conditions, shape factor b

$$b = 0.85 \qquad h_t^2/(H_{m0}L_{m-1,0}) \leq 0.23 \tag{6}$$

To estimate, the scale factor, a, EurOtop (2016) proposed the following empirical formula (Equation 7) with an empirical relationship between $\Gamma(1 + 1/b)$ and shape factor b, see EurOtop (2016) for details.

$$a = \left(\frac{1}{\Gamma\left(1 + \frac{1}{b}\right)}\right)\left(\frac{qT_m}{P_{ov}}\right) \tag{7}$$

where, Γ is the mathematical gamma function, q is the mean overtopping discharge per m width (m^3/s per m or l/s per m) and P_{ov} is the proportion of overtopping waves (N_{ow}/N_w).

For a known relative crest freeboard (R_c/H_{m0}), EurOtop (2016) proposed the following empirical formulas (Equation 8 and 9) to determine the proportion of overtopping waves (P_{ov}) at a plain vertical wall under perpendicular wave attack, subjected to non-impulsive and impulsive wave conditions.

For non-impulsive conditions ($h_t^2/(H_{m0}L_{m-1,0}) > 0.23$), P_{ov}

$$P_{ov} = \frac{N_{ow}}{N_w} = \exp\left[-1.21\left(\frac{R_c}{H_{m0}}\right)^2\right] \tag{8}$$

For impulsive conditions ($h_t^2/(H_{m0}L_{m-1,0}) \leq 0.23$), P_{ov}

$$P_{ov} = \frac{N_{ow}}{N_w} = 0.024\left[\frac{h_t^2}{(H_{m0}L_{m-1,0})}\left(\frac{R_c}{H_{m0}}\right)\right]^{-1} \text{ with a minimum predicted by Equation 8} \tag{9}$$

2.2 Empirical predictions of toe scour

A number of researchers reported that the failure of coastal structures such as seawalls in the UK very often occurred due to the scour at the toe of the structure, see Sutherland et al. (2003). To improve understanding of this phenomenon as well as to provide design guidance, many experimental and field studies, have focused on toe scouring at coastal structures with sandy foreshores, for example; Xie (1981); Fowler (1992); Kraus and Smith (1994); Sutherland et al. (2006); Tsai et al. (2009); Pearce et al. (2006). An overview of laboratory and field research on toe scouring at vertical structures using sandy beach profiles is summarized by Müller et al. (2008). Alongside experimental studies, a few numerical studies have been performed to understand the scouring patterns at coastal structures, for example Jayaratne et al., (2016); Pourzangbar et al., (2017); Tahersima et al., (2011); Tofany et al., (2014).

It has been noted in the literature by many researchers that there is a strong correlation between the toe scour depth and relative water depth at the structure. For example, Müller et al. (2008) illustrated a trend line describing the development of non-dimensional toe scour depth (S_t/H_s) with respect to the breaker type (h_b/L_m) for the vertical seawalls on a sandy beach. Further, Sutherland et al. (2008) and Wallis et al. (2009) demonstrated a new empirical relationship between non-dimensional toe scour depth (S_t/H_s) and relative toe water depth (h_t/L_m), for the conservative prediction of scour depth at a plain vertical seawall with a sandy foreshore slope. In which, H_s significant wave height defined as highest one-third of wave heights = $H_{1/3}$, h_t is the toe water depth, h_b is the water depth at breaking and L_m is the deep-water wave length based on mean wave period T_m.

With prototype sedmiment diamaters of $5 < d_{50} < 30$ mm, and a model scale of 1:17, Powell and Lowe (1994) derived a non-dimensional scour plot for the estimation of toe scouring depth at vertical walls with a permeable shingle beach under normally incident irregular wave attack.

Jayaratne et al. (2015) conducted a laboratory study on scouring at vertical seawall with a sandy slope, and two gravel slopes. They suggested an empirical model for the estimation of scour depth, using the maximum wave height at the toe of the slope, submergence of the berm and local wave length. However, to date these empirical models, together with new datasets have not been validated with experimental data.

3. Experimental Set-Up

3.1 Laboratory description

Physical model experiments were undertaken in a 2D wave flume within the school of engineering at the University of Warwick. The wave channel has a length of 22 m, a width of 0.60 m and an operating depth of 0.40 m - 0.70 m. The sidewalls and bottom of the wave flume are built of glass. The flume is equipped with an absorbing piston type wavemaker to generate regular as well as random waves.

A 1:50 length scale was applied to generate random sea wave conditions within the flume. A sloping beach with a uniform slope of 1:20 was constructed in front of the vertical seawall to generate depth limited waves. A smooth impermeable slope was constructed to perform the experiments with a solid beach. A permeable shingle beach was made of scaled anthracite to conduct the experiments for the shingle beach configurations, see Fig. 1.

All measurements were undertaken with a model vertical seawall. For the experiments on mobile shingle beds, two shingle beaches were designed and represented by filtered anthracite crushed coal with a specific gravity of 1.40. The scaling of mobile shingle beaches was applied, by adapting the well-established methodology of Powel (1990). For the selection of model beach sediment in laboratory investigations, Powel (1990) described that model sediment should satisfy the following three criteria:

— In physical model tests, permeability should be accurately reproduced to reach the real beach slope

— The correct reproduction of the relative magnitudes of the onshore and offshore movement to evaluate whether the erosion or accretion will occur at the beach

— To identify the minimum wave velocity for initiating the motion of the beach, the threshold of movement should be correctly scaled in the experiments

Powell (1990) applied the methods published by Yalin (1963), Dean (1973) and Komar and Miller (1973) to satisfy the permeability, onshore and offshore movement and, threshold of movement criteria respectively. Adopting the method described by Powel (1990), at a 1:50 scaling, model beach materials d_{50} of 2.10 mm and 4.20 mm with a specific gravity of 1.40 T/m^3 were designed to represent assumed prototype grain diameter d_{50} of 13 mm and 24 mm respectively with a specific gravity of 2.65 T/m^3. The grading curves of model beach sediments in this study are shown in Fig. 1. To avoid confusion, any reference to the sediment within this manuscript has been quoted as prototype values.

a.

b.

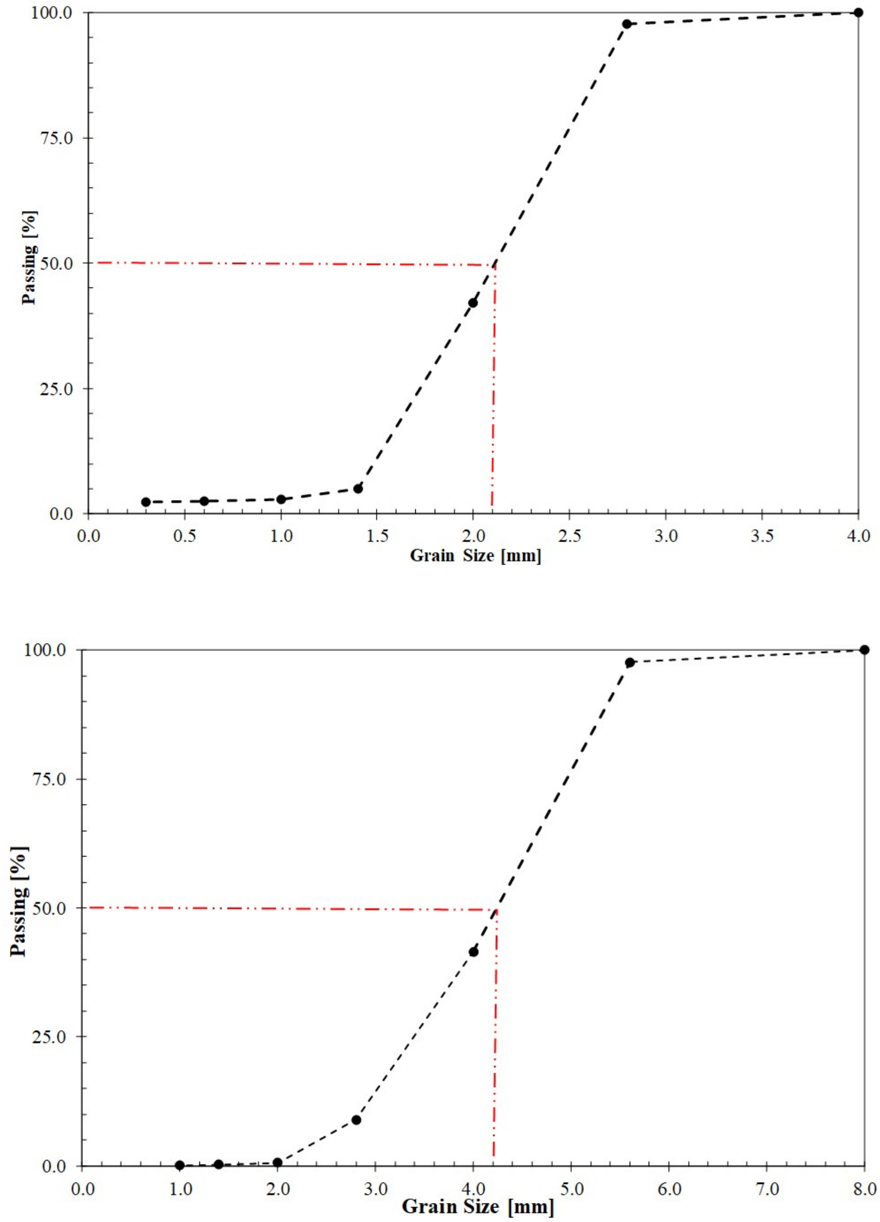

Fig. 1. The grading curves of model beach sediments - a) d_{50} of 2.10 mm b) d_{50} of 4.20 mm

3.2 Measurement of wave conditions

The wave heights and periods were calculated by collecting free water surface elevations at the different points during the experiments. To separate the incident and reflected condition, a 3-point method was applied to determine the wave conditions at the structure as well as at deep water (near wave paddle), see Mansard and Funk (1980). To determine the deep water wave conditions, one set of three wave gauges (number 1, 2 and 3) were positioned near wave paddle at relatively deep water, see Fig. 2. The water surface elevations at the structure were measured by placing another set of three wave gauges (number 4, 5 and 6 in Fig. 2) close to the structure. The probe spacing between wave gauges was calculated as following the approach prescribed by Mansard and Funk (1980). The wave gauge (number 6, see Fig. 2) in front of the vertical seawall was positioned at 750 mm (0.25 times of wave length associated with peak frequency and local water depth) from the face of the structure. This was executed using the methodology described by Klopman and Van der Meer (1999) which enables to avoid the effects of a reflective structure on incident significant wave heights. These authors found that for the vertical walls there is limited influence of the structure on the incident significant wave heights thus it is possible to place the multi-gauge wave measurement method adjacent to the structure. This is because vertical structure is almost near to a perfectly reflective wall thus as per linear wave theory “there are no evanescent wave modes only the incident and reflecting travelling waves are present” (Klopman and Van der Meer, 1999).

To compensate the reflected waves originating from the structure, the wave paddle was equipped with an active absorption system during the overtopping and scouring tests. Furthermore, the incident wave conditions were calibrated by repeating the test sequence without the presence of structure, which enables the effects of wave-structure induced reflection to be evaluated.

3.3 Measurement of overtopping

To collect and measure the overtopping discharges, an overtopping measuring container was placed on the rear side of the structure, connected with an overtopping chute from the crest of structure. For the tested conditions on the shingle beach, a perforated sheet made of stainless steel was positioned on the upper side of container to collect the overtopped sediment particles. The diameter of the hole of the perforated sheet was smaller than the diameter of model shingle beach which enables the overtopped sediments to be separated from the water. A suction pump was attached with the measuring container to empty it after or during a test run. The container was suspended from a load-cell that allows the measurement of overtopping mass as a form of change in voltage for each overtopping event, during the experimental test sequence. The calibration of load-cell was performed by measuring the change in voltage in the loadcell corresponding to known change in weights in the container.

Further, to detect an overtopping event, an overtopping detector was made with the use of two parallel metal strips of metal tape setting along the crest of seawall. During an overtopping event, water overtops the crest of structure and goes through the metal strips, which is configured to show a voltage drop, as the overtopped wave passes the strips. Thus, allowing identification of every wave-by-wave overtopping volume during each test.

The load-cell and overtopping detector were connected with a data logger to process and store all the output signals at a desired frequency of 20 Hz. At the end of the experiment, collected data were passed through an algorithm to determine the total overtopping volume and the wave by wave overtopping volumes for an experiment.

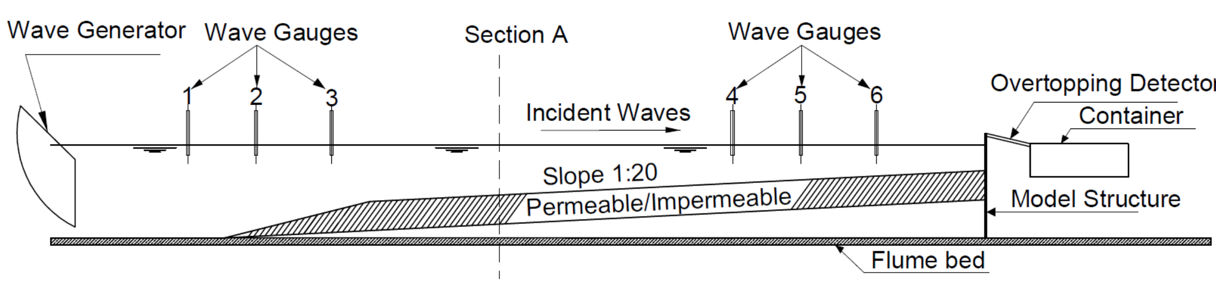

a.

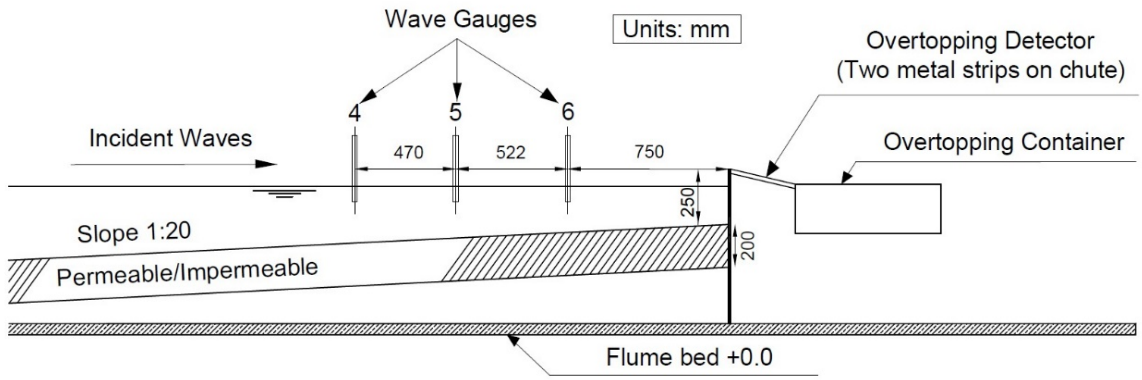

b.

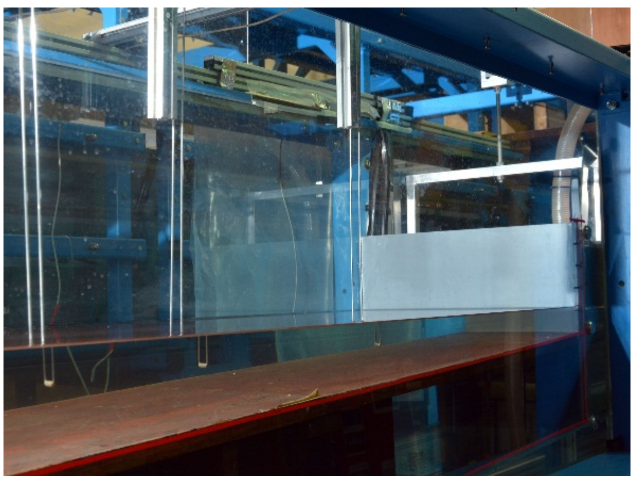

c.

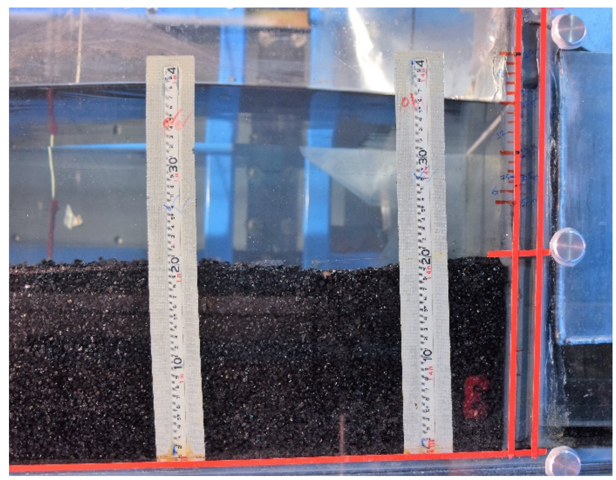

d.

Fig. 2. Test set –up: a. A layout of the physical model, b. Detail of the position of wave gauges and overtopping measurement system (Section A), c. Photograph of impermeable bed configuration and d. Photograph of shingle bed (d_{50} = 13 mm) configuration

3.4 Measurement of scouring

Measurements of toe scouring and wave overtopping were conducted simultaneously for tests on plain vertical seawalls with a shingle foreshore. Due to the simultaneous measurements of overtopping and toe scouring, all the tests were performed with 1000 random waves and the scour depth was also calculated for 1000 wave cycles. Prior to the start of each experiment, the shingle bed was reshaped to the initial profile which was uniform 1:20 permeable foreshore slope in front of the vertical wall.

A depth point gauge was used to measure the scour depths at the end of the test. For each experiment, scour depth at toe (S_t) and maximum scour depth (S_{max}) were measured after a test run. For selected conditions, scour depths were also measured at several locations along the shingle bed to determine the bed profile of shingle beach after wave attack. This was performed using the depth point gauges at defined locations as well as a digital camera from a fixed position and subsequent analysis was applied.

3.5 Test conditions

In general, for a wind sea state wave steepness varies from s_{op} = 0.04 to s_{op} = 0.06 and for swell wave conditions it is usually s_{op} = 0.01 (EurOtop, 2016). To generate both wind sea state and swell sea conditions, two constant wave steepnesses (s_{op}= 0.02 and 0.05) in relatively deep water were tested in this study. The incident wave conditions at the toe of the structure is presented in Table 1.

The JONSWAP energy spectrum is usually applied as the design spectrum by coastal engineers (Holthuijsen, 2007) and employed in experimental studies by researchers for enabling comparison of gathered data. The mean values of shape parameters for the JONSWAP energy spectrum, are $\gamma = 3.3$, $\sigma_a = 0.07$ and $\sigma_b = 0.09$ (Holthuijsen, 2007; Wolters et al., 2009). To generate a realistic irregular wave field, a JONSWAP energy spectrum was used in this study with a peak enhancement factor of $\gamma = 3.3$ ($\sigma_a = 0.07$ and $\sigma_b = 0.09$).

Table 1

Summary of test conditions

Structural configuration	Bed configuration	Toe water depth, h_t [m]	Crest Freeboard, R_c [m]	Wave Height, H_{m0} [m]	Wave steepness, s_{op} [-]	Wave Period, $T_{m-1,0}$ [s]
Vertical Seawall on an impermeable bed	solid	0.060	0.190	0.05-0.16	0.02	1.27-2.26
					0.05	0.80-1.43
	solid	0.075	0.245	0.05-0.16	0.02	1.27-2.26
					0.05	0.80-1.43
	solid	0.100	0.150	0.05-0.16	0.02	1.27-2.26
					0.05	0.80-1.43
	solid	0.150	0.100	0.05-0.16	0.02	1.27-2.26
					0.05	0.80-1.43
	solid	0.180	0.140	0.05-0.16	0.02	1.27-2.26
					0.05	0.80-1.43
	solid	0.200	0.050	0.05-0.16	0.02	1.27-2.26
					0.05	0.80-1.43
Vertical Seawall on a shingle bed	shingle (d_{50} = 13 mm & 24 mm)	0.060	0.190	0.05-0.16	0.02	1.27-2.26
					0.05	0.80-1.43
	shingle (d_{50} = 13 mm & 24 mm)	0.075	0.245	0.05-0.16	0.02	1.27-2.26
					0.05	0.80-1.43
	shingle (d_{50} = 13 mm & 24 mm)	0.100	0.150	0.05-0.16	0.02	1.27-2.26
					0.05	0.80-1.43
	shingle (d_{50} = 13 mm & 24 mm)	0.150	0.100	0.05-0.16	0.02	1.27-2.26
					0.05	0.80-1.43
	shingle (d_{50} = 13 mm & 24 mm)	0.180	0.140	0.05-0.16	0.02	1.27-2.26
					0.05	0.80-1.43
	shingle (d_{50} = 13 mm & 24 mm)	0.200	0.050	0.05-0.16	0.02	1.27-2.26
					0.05	0.80-1.43
	shingle (d_{50} = 13 mm & 24 mm)	- 0.050		0.05-0.16	0.02	1.27-2.26
					0.05	0.80-1.43
	shingle (d_{50} = 13 mm & 24 mm)	- 0.030		0.05-0.16	0.02	1.27-2.26
					0.05	0.80-1.43

For this study, a matrix of 180 test conditions (wave steepnesses, crest freeboards, water depths, shingle sizes) were performed to investigate the wave overtopping at vertical walls on both impermeable and shingle beaches. In total, six depths within the water column at the toe of the structure, were tested to examine the wave overtopping and toe scouring at vertical walls on shingle beaches. In addition, tests were conducted with negative toe water depths (water depth below beach level) to investigate the toe scouring at vertical seawalls with a shingle foreshore. An overview of test conditions is presented in Table 1.

4. Results and Discussion

4.1 Wave overtopping

Mean overtopping discharge

The experiments were benchmarked with an impermeable foreshore, subjected to both non-impulsive and impulsive conditions.

In Fig. 3, the resulting mean overtopping discharges at a plain vertical wall on shingle beds are compared with the empirical formulae (Equation 2-3) proposed by EurOtop (2016), together with overtopping characteristics observed for the reference case (solid bed). The resulting data points, which correspond to the solid impermeable bed, show an overall very good agreement with the predictive method of EurOtop (2016) as observed by dotted lines in Fig. 3 (R^2 = 0.88). For the impulsive conditions tested on the shingle beaches, a noticeable reduction on the mean overtopping rate is observed compared to the test results on an impermeable bed. When comparing the two beach foreshore configurations, it was observed that the larger shingle bed of d_{50} of 24 mm, gave a greater overall reduction in overtopping discharge, as indicated by the dashed trend lines.

It is noticeable from Fig. 3, that experiments with shingle foreshores give more scatter compared to the impermeable bed configurations, subjected to impulsive wave attack. The higher scatter values of relative overtopping discharge are observed for the data points corresponding to low overtopping waves (less than 5%), see Fig. 3. These are often associated with a very few number of overtopped waves, leading to an uncertainty in the measurement of wave overtopping. Similar scatter characteristics of wave overtopping for experiments with less than 5% overtopping waves, were also reported by Zanuttigh et al. (2013) in the determination of wave by wave overtopping characteristics for smooth slopes and rubble mound breakwaters.

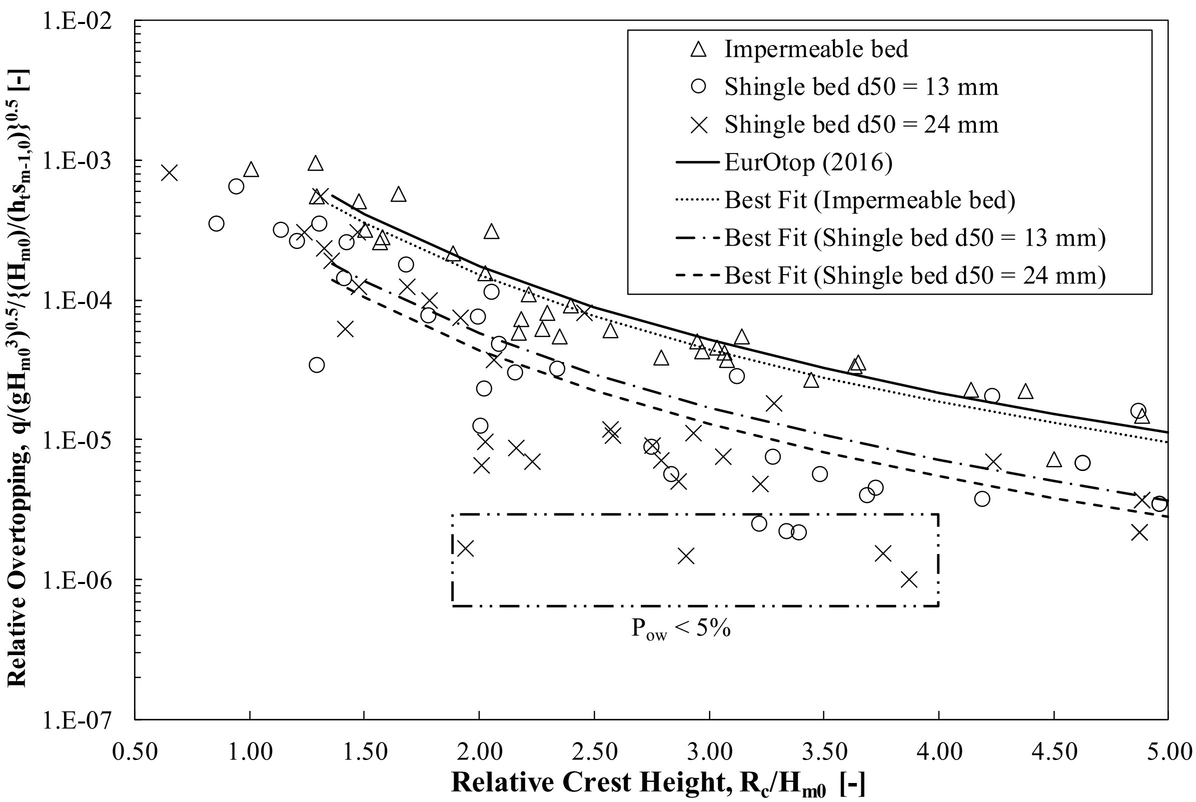

Fig. 3. Mean overtopping discharge at plain vertical walls, subjected to impulsive conditions

A 'best-fit' analysis was performed on the measured overtopping data to determine a reduction factor by introducing mobile beds and to propose the empirical overtopping discharge formula for the estimation of mean overtopping at vertical seawalls on a shingle foreshore. Following the approach suggested by EurOtop (2016), for higher freeboards with impulsive wave conditions, average overtopping discharges at vertical walls on the mobile beds are described by a power law function. Based on the 'best-fit' analysis on the tested conditions, the overtopping rate is reduced by around a factor of 3 for shingle bed of d_{50} of 13 mm (Equation 10) and approximate factor of 4 for shingle bed of d_{50} of 24 mm (Equation 11), when compared to the empirical prediction of EurOtop (2016) for solid impermeable bed (Equation 3). It should be noted that for lower relative freeboards (R_c/H_{m0}<1.35) less data was collected for impulsive conditions, thus it is not possible to give a defined trend through the best-fit analysis.

Alongside the R^2 best-fitted analysis, the root mean square error (rmse) analysis has been carried out in this study, to observe the reliability of the best-fitted equations. This has been performed by adopting the methodologies of Owen (1980) and Victor et al. (2012), using measured and predicted values of mean overtopping discharges. For the tested impulsive conditions, the rmse value based on the measured, and predicted values of average overtopping rates was derived, with values of 0.25 and 0.28, for shingle beds of d_{50} = 13 mm and d_{50} = 24 mm respectively. It is important to note that the scatter data points which are the experiments with relatively low overtopping (less than 5%) as indicated in Fig. 3, are not considered in the rmse analysis of new equations.

The best-fit trend line for shingle bed of d_{50} = 13 mm (Impulsive conditions),

$$\frac{q}{\sqrt{gH_{m0}^3}} = 0.00046\ (\frac{H_{mo}}{h_t s_{m-1.0}})^{0.5}\ (\frac{R_c}{H_{mo}})^{-3.0} \qquad \text{for } 1.35 \leq \frac{R_c}{H_{m0}} \leq 5.0 \tag{10}$$

With a corresponding least square regression, R^2 = 0.63 and rmse value of 0.25.

The best-fit trend line for shingle bed of d_{50} = 24 mm (Impulsive conditions),

$$\frac{q}{\sqrt{gH_{m0}^3}} = 0.00035\,(\frac{H_{mo}}{h_t s_{m-1.0}})^{0.5}\,(\frac{R_c}{H_{mo}})^{-3.0} \qquad \text{for } 1.35 \le \frac{R_c}{H_{m0}} \le 5.0 \tag{11}$$

With a corresponding least square regression, $R^2 = 0.54$ and rmse value of 0.28.

Fig. 4 illustrates a comparison between the mean overtopping discharge for the shingle bed and impermeable solid bed configurations, under non-impulsive wave conditions. The empirical predictions (Equation 1) by new overtopping manual (EurOtop, 2016) is presented by a solid line. The data points corresponding to solid impermeable bed show an overall good agreement with the predictive method of EurOtop (2016), as indicated by dotted lines in Fig. 4 ($R^2 = 0.96$ and rmse value of 0.09). For the non-impulsive test conditions on shingle beaches, the results of this study demonstrate that permeable shingle foreshore provides a reduction in the overtopping discharge at vertical seawalls, compared to an impermeable beach configuration.

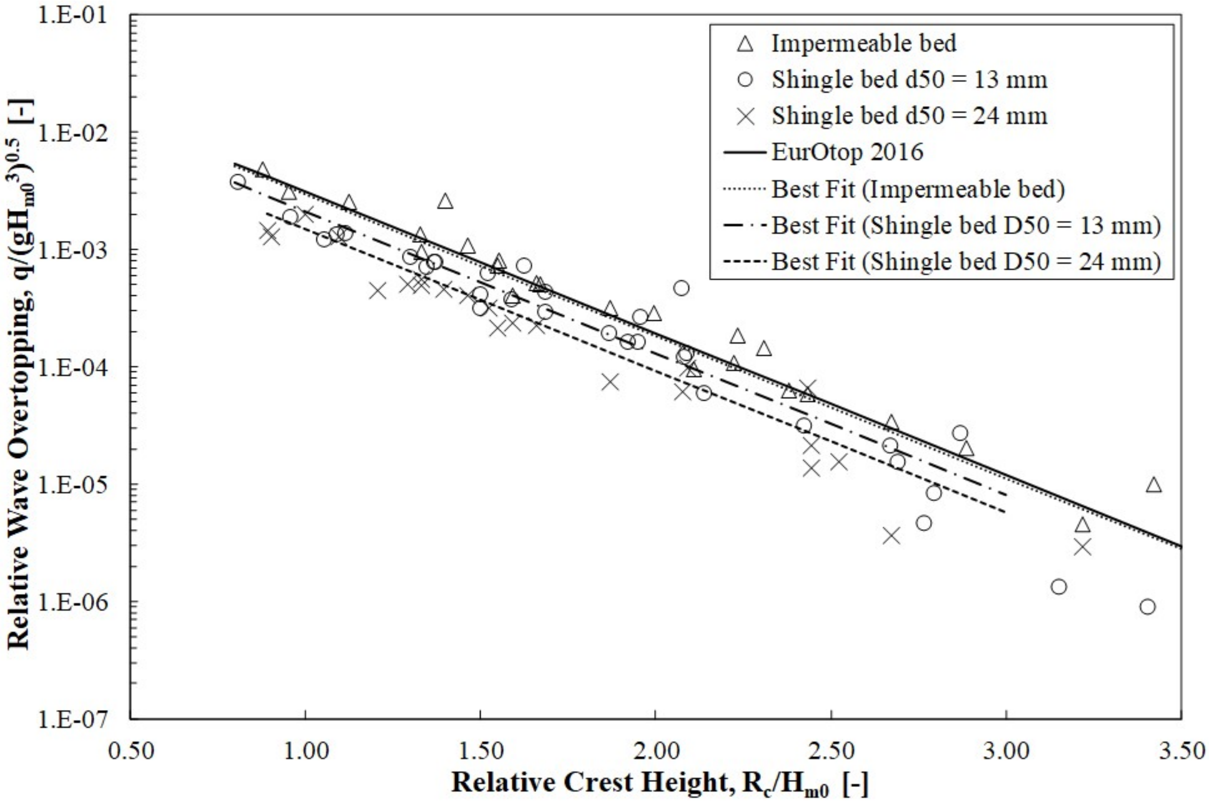

Fig. 4. Mean overtopping discharge at plain vertical walls, subjected to non-impulsive conditions

A ‘best-fit’ analysis was carried out on the shingle bed data under non-impulsive conditions on the overtopping discharge trend curve for a plain vertical wall with a permeable shingle foreshore, see Equation 12-13. When compared to the empirical prediction of EurOtop (2016) for solid impermeable beaches (Equation 1), it appears that under non-impulsive conditions, the mean overtopping discharge is reduced by approximately a factor of 1.5 for shingle bed of d_{50} of 13 mm (Equation 12) and around a factor of 2 for shingle bed of d_{50} of 24 mm (Equation 13). It should be noted that the scatter data points corresponding to relative freeboards higher than 3.5 are not considered in the ‘best-fit’ analysis. The rmse value is reported as only 0.10 and 0.11 for shingle bed of d_{50} = 13 mm and d_{50} = 24 mm respectively, despite the larger scatter, in general the predictions with the use of the new equations show an encouraging trend with the measurements.

The best-fit trend line for shingle bed of d_{50} = 13 mm (non-impulsive),

$$\frac{q}{\sqrt{gH_{m0}^3}} = 0.033 \exp\left(-2.77\frac{R_c}{H_{m0}}\right) \tag{12}$$

With a corresponding least square regression, $R^2 = 0.92$ and rmse value of 0.10.

The best-fit trend line for shingle bed of d_{50} = 24 mm (non-impulsive),

$$\frac{q}{\sqrt{gH_{m0}^3}} = 0.024 \exp\left(-2.91\frac{R_c}{H_{m0}}\right) \tag{13}$$

With a corresponding least square regression, $R^2 = 0.94$ and rmse value of 0.11.

Mean overtopping sediment discharge

For the experiments with the mobile shingle beds, alongside the mass of overtopped water, the mass of overtopped sediment was simultaneously measured to determine the average overtopping sediment discharge. The quoted specific gravity of 1.40 was used to determine the volume of overtopped sediments from collected dry weight of sediments. Fig. 5 shows the measured average overtopping rate of sediment and water at a plain vertical wall on a shingle foreshore, plotted against the relative freeboard of the structure, subjected to impulsive wave conditions. It should be noted that the overtopping of sediment was not observed for the tested conditions on non-impacting and impacting waves ($h_t^2/(H_{m0}L_{m-1,0}) > 0.03$). Overall, the data points in Fig. 5 demonstrate that measured volume of sediment passing the crest of the structure is around 0.5% of the volume of overtopped water, for the conditions where $h_t^2/(H_{m0}L_{m-1,0}) < 0.03$. For instance, if considering the relative freeboard of 2.01 for shingle bed of 24 mm, it is noticeable that the dimensionless sediment discharge (1.83E-07) is 0.41% of the overtopped water (4.50E-05).

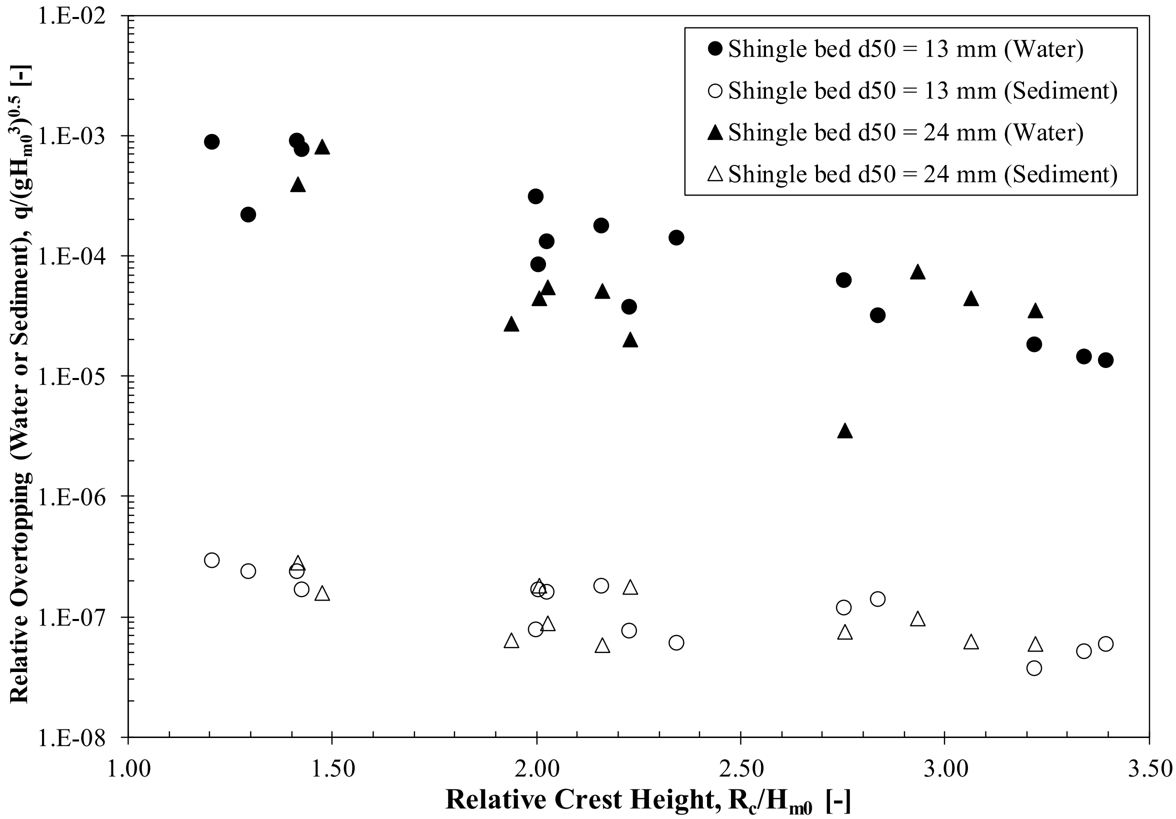

Fig. 5. Mean overtopping discharge of sediment and water at a plain vertical wall with a shingle foreshore

Distribution of wave by wave volumes

In the empirical prediction of overtopping volumes, it is generally considered that the wave by wave overtopping volumes in a sequence follow a two parameter Weibull distribution (Van der Meer and Jansen, 1994; Besely, 1999; EurOtop, 2016). For this study, wave by wave overtopping volumes were measured and plotted on a Weibull scale for each experiment to identify the distribution of these volumes. For three different tested bed configurations with the same wave conditions, distribution of wave by wave volumes on a Weibull scale are presented in Fig. 6, where V is the individual overtopping volume, $P(V)$ is the probability of exceedance and V_{bar} is the mean overtopping volume. Fig. 6 also compares the variation of overtopping volume distribution for three different bed configurations.

Overall, a linear trend of data points is noticeable from graphs (Fig. 6a -6c), which denotes that the measured individual overtopping volumes fit a two-parameter Weibull distribution for the tested conditions within this study. Furthermore, the graph (Fig. 6d) also demonstrate that there is no apparent effect of permeable foreshores on the distribution of wave by wave volumes.

In the Weibull distribution of wave by wave volumes, distributions of the small overtopping volumes (lower part) in many cases deviate from the inclination of the upper part of the distribution (Victor et al., 2012; Zanuttigh et al., 2013). Many researchers reported that higher wave by wave volumes give a good fit to Weibull distribution and provide a reliable estimation of extreme individual overtopping wave volumes, see Van der Meer and Janssen (1994) and Besley (1999). Generally, practitioners mainly focus on the largest wave overtopping volumes, hence Zanuttigh et al. (2013) suggested to use the upper part of distribution to get a good fit at the extreme overtopping wave volumes. Adopting the procedure of Pearson et al. (2002), the best-fit linear trend line in Fig. 6 is plotted by considering only the upper part of the resulting distribution of wave by wave volumes. The shape factor b of the distribution can be determined from the inclination of best fitting line.

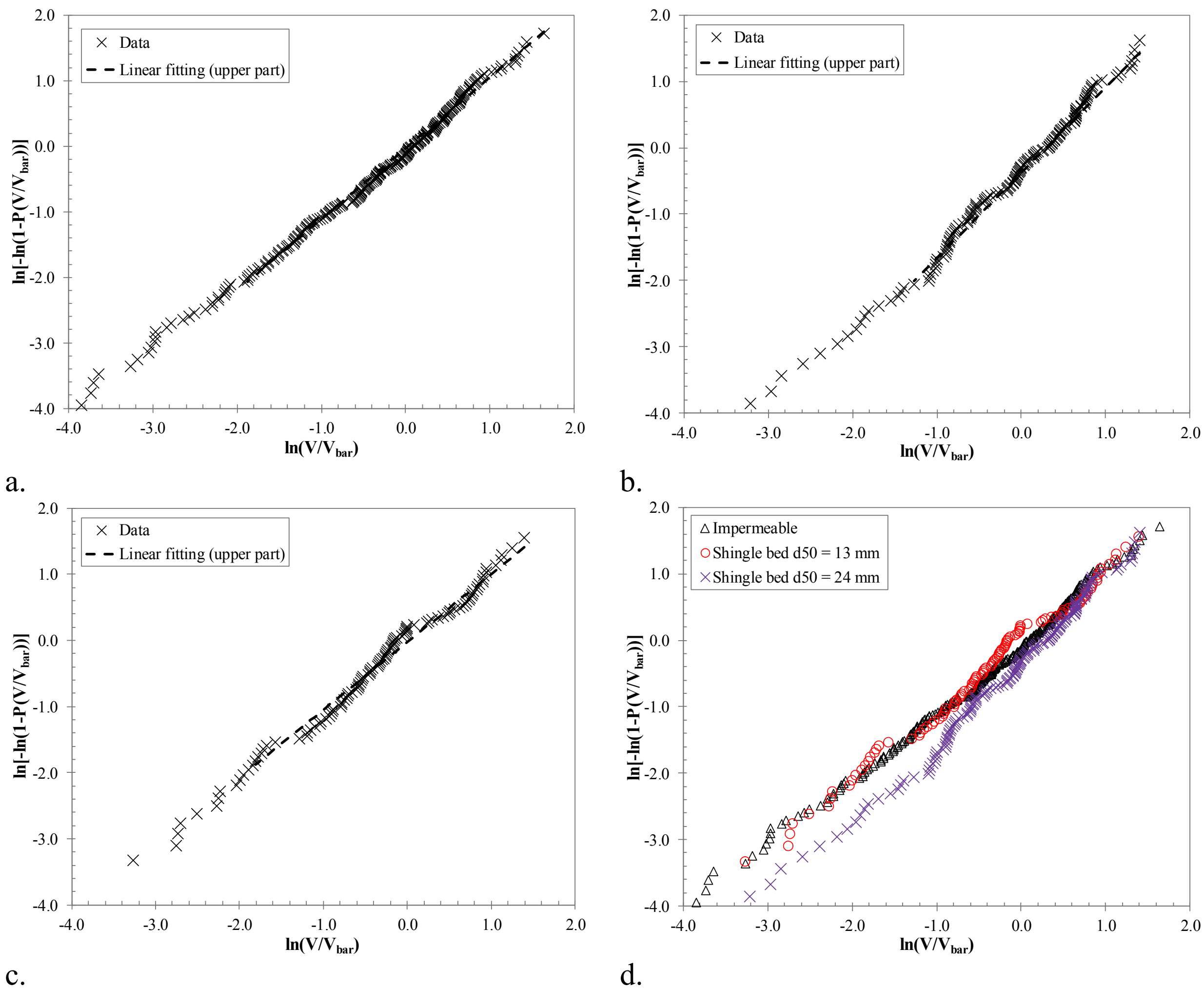

Fig. 6. Distribution of measured wave by wave overtopping volumes for $s_{m-1,0} = 0.06$, $H_{m0} = 0.10$ m - a) Impermeable bed b) Shingle bed $d_{50} = 24$ mm and c) Shingle bed $d_{50} = 13$ mm and d) Variation of wave by wave volumes with different bed configurations

Maximum individual overtopping volume

In Fig. 7, the measured maximum individual overtopping wave volumes (V_{max}) at plain vertical walls on a solid impermeable bed are compared with those predicted values using empirical prediction (Equation 4) proposed by EurOtop (2016). The graph also compares the measured maximum individual overtopping wave volumes at plain vertical walls on the shingle beds with the empirical predictions suggested by EurOtop (2016) for both impulsive and non-impulsive conditions. For both shingle and solid beds, the maximum individual overtopping wave volumes were predicted using the empirical formula (Equation 4) for vertical walls given by new overtopping manual EurOtop (2016). Overall, the data points corresponding to impermeable beach demonstrate that measured maximum individual volume, V_{max} correlates reasonably well (within a factor 2) with the predicted maximum individual overtopping wave volumes under both impulsive and non-impulsive wave conditions.

In general, the maximum individual wave by wave volumes are somewhat lower than the predicted values by EurOtop (2016). Nevertheless, due to the scatter characteristics of the data points, it can be concluded that there is no significant difference in the estimation of wave by wave volumes for solid and shingle beds in front of a plain vertical seawall.

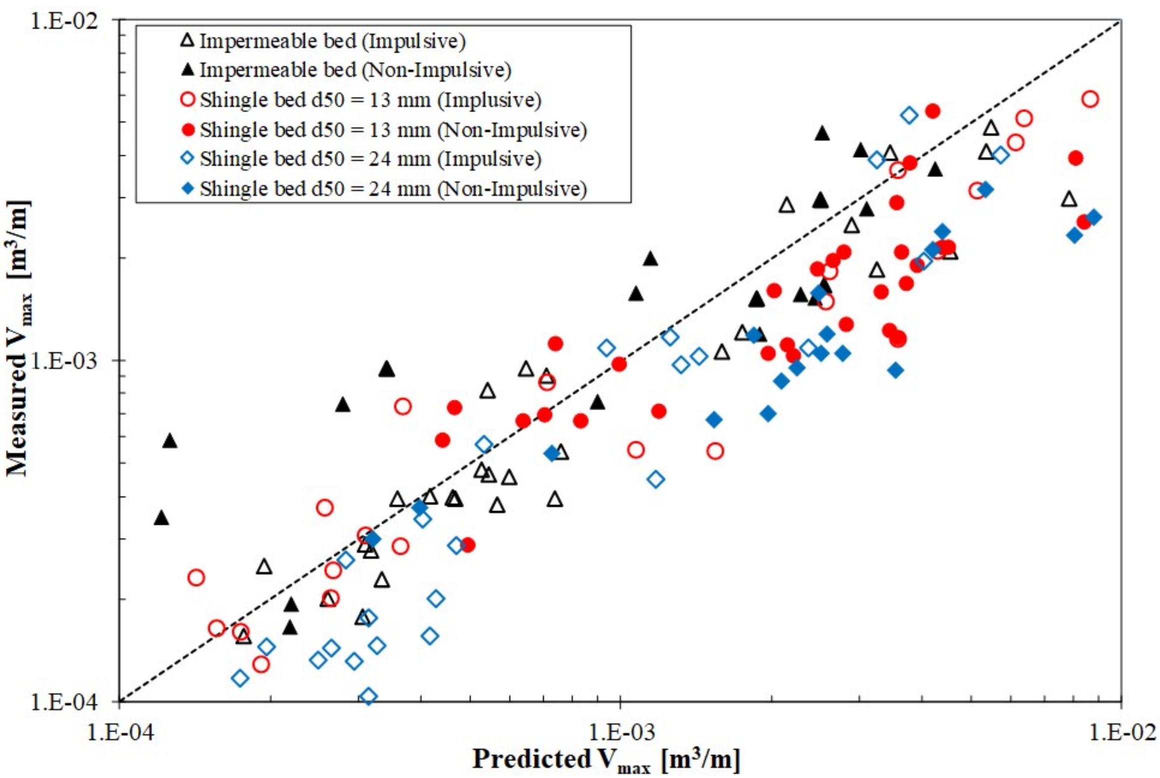

Fig. 7. Comparison of measured and predicted individual overtopping volumes at plain vertical walls on solid and shingle foreshores

Proportion of overtopping waves

Fig. 8 shows the comparison between the measured proportion of overtopping waves at vertical walls for both solid and shingle beds with the empirical predictions reported by EurOtop (2016). The results from the benchmark tests (solid impermeable foreshore) are plotted in Fig. 8, as the reference case. The percentage of waves overtopping predicted with the use of new empirical formulae (Equation 8-9) and plotted in Fig. 8 by six different lines showing six values of impulsiveness parameter $(h_t^2/(H_{m0}L_{m-1,0}))$. The solid black line $(h_t^2/(\mathrm{H_{m0}}L_{m-1,0}) = 0.24)$ represents the estimated proportion of overtopping waves for non-impulsive wave conditions reported by EurOtop (2016) for plain vertical walls.

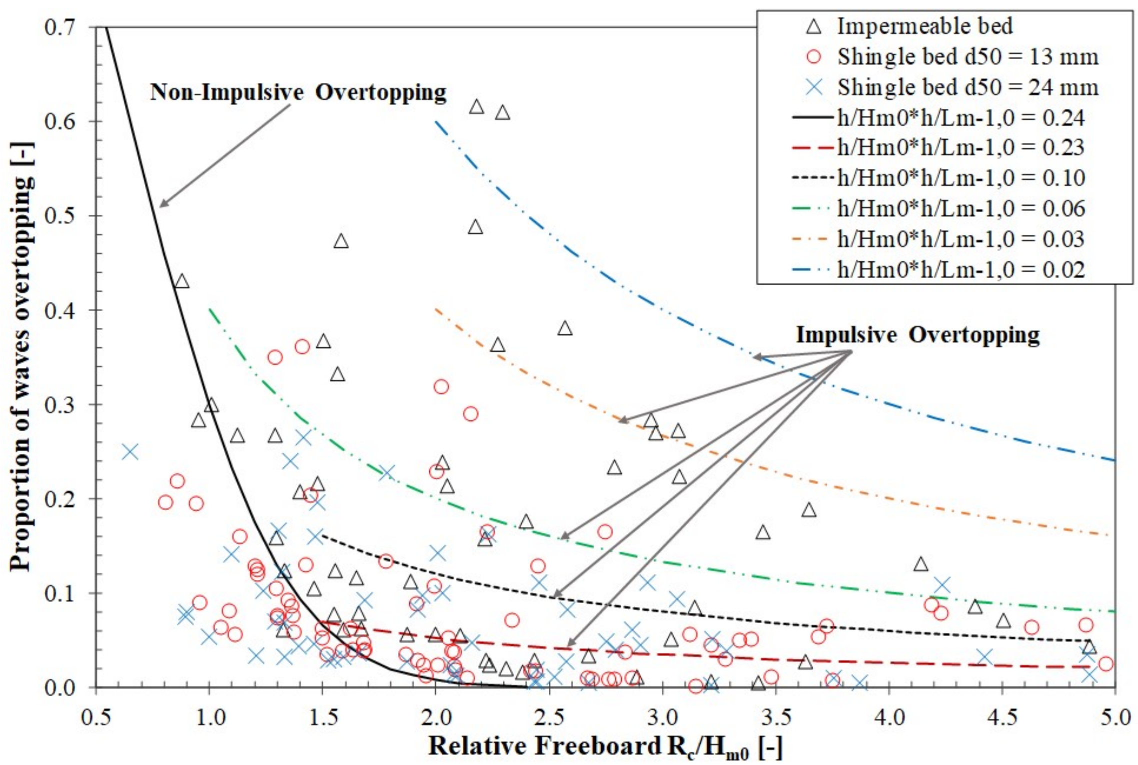

Fig. 8. Proportion of waves overtopping at plain vertical walls for both solid and shingle beach configurations, compared to empirical prediction

The results show that for the tested conditions on the solid impermeable bed, the measured data points approximately follow the trend of that described by EurOtop (2016). However, for the shingle foreshore configurations, it is observed that that probability of overtopping decreases, indicating that the porosity of the shingle beds has an influence on the proportion of overtopping waves. For instance, the data points corresponding to experiments with shingle beach of d_{50} of 24 mm give larger reduction in overtopping proportions compared to data points of shingle beach of d_{50} of 13 mm.

4.2 Toe scouring

For this study, the initial bed profile was 1:20 plain permeable shingle beach. As noted previously, tests were performed for 1000 irregular wave cycles, and simultaneous measurements of overtopping and toe scouring, were measured. To investigate development time for maximum toe scour depth, an initial selection of experiments was also undertaken for 3000 irregular waves, with scour depths measured, after approximately 1000, 2000 and 3000 wave cycles. Fig. 9 shows the measured scour depth, plotted against number of wave cycle. The results show that the maximum scour depth, occurred at around 1000 wave cycles. Hence the scour depth at 1000 waves, was adopted for all measured conditions, as the maximum scour depth.

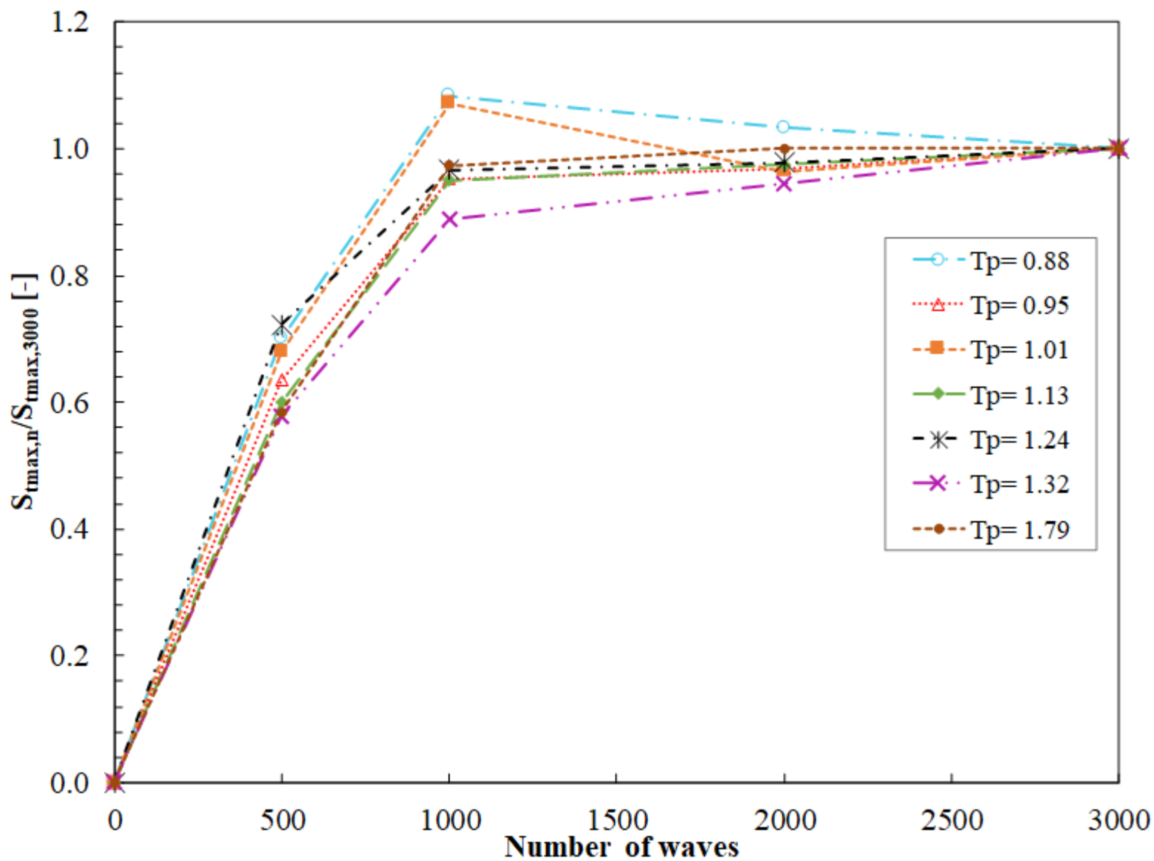

Fig. 9. Time development of maximum scour depth

Bed level changes for a vertical wall with a shingle foreshore

Fig. 10 shows the observed bed level changes (final – initial elevation of bed) after 1000 random waves for both swell and storm sea state. In Fig 10, negative values of bed level changes represent scour while positive values denote accretion. All the tests were performed with same initial bed profile (1:20 uniform shingle bed) and same wave conditions but with different toe water depths (h_t = 0.18 m, h_t = 0.16 m, h_t = 0.15 m, h_t = 0.10 m, h_t = 0.075 m and h_t = 0.06 m). It should be noted that experiments with nominal wave steepness (s_{op}) of 0.02 and 0.05 were designed to replicate swell sea conditions and storm sea state respectively. The results of this study demonstrate that for any given relative toe water depth, accretion at the toe of the structure was reported for swell sea state whereas scouring was noted for wind sea state. This can be also related with reality where accretion at the structure is mostly observed for swell sea state and scouring under storm sea conditions.

Furthermore, it can be also observed from Fig 10 that for any given wave conditions, the maximum accretion or scouring occurs for lowest toe water depth. For instance, all the tests in Fig. 10(a) were performed with a nominal wave steepness of 0.02 and with significant wave height (H_{m0}) of 0.085 m but with six different toe water depths. The test results showed that maximum accretion (0.081 m) at the structure occurred for lowest toe water depth of 0.06 m, see Fig. 10(a).

a.

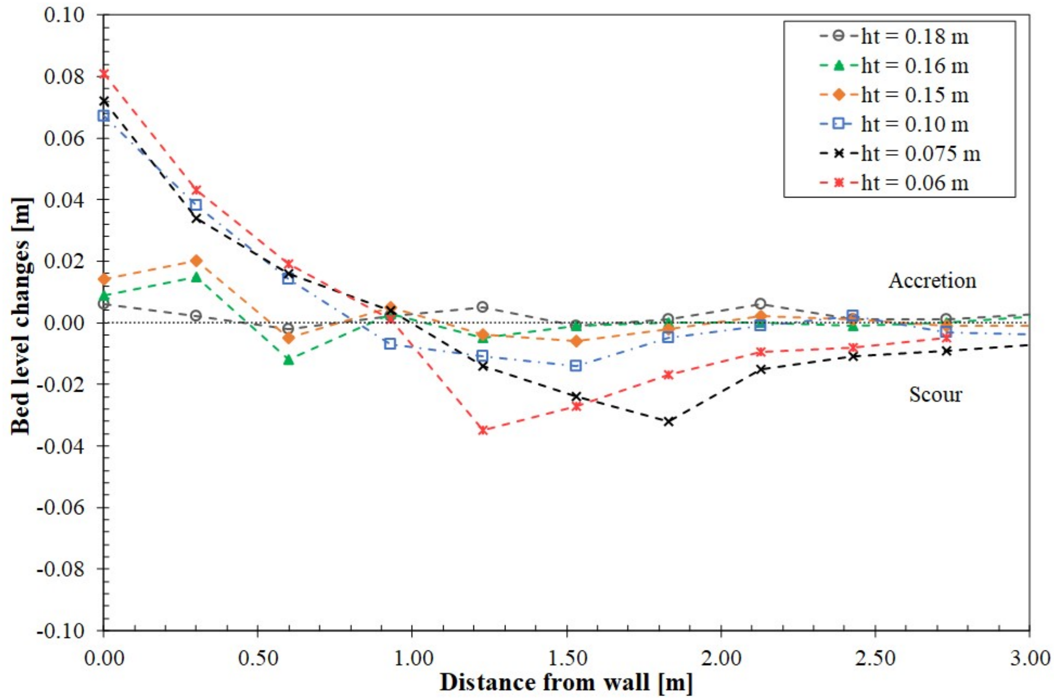

b.

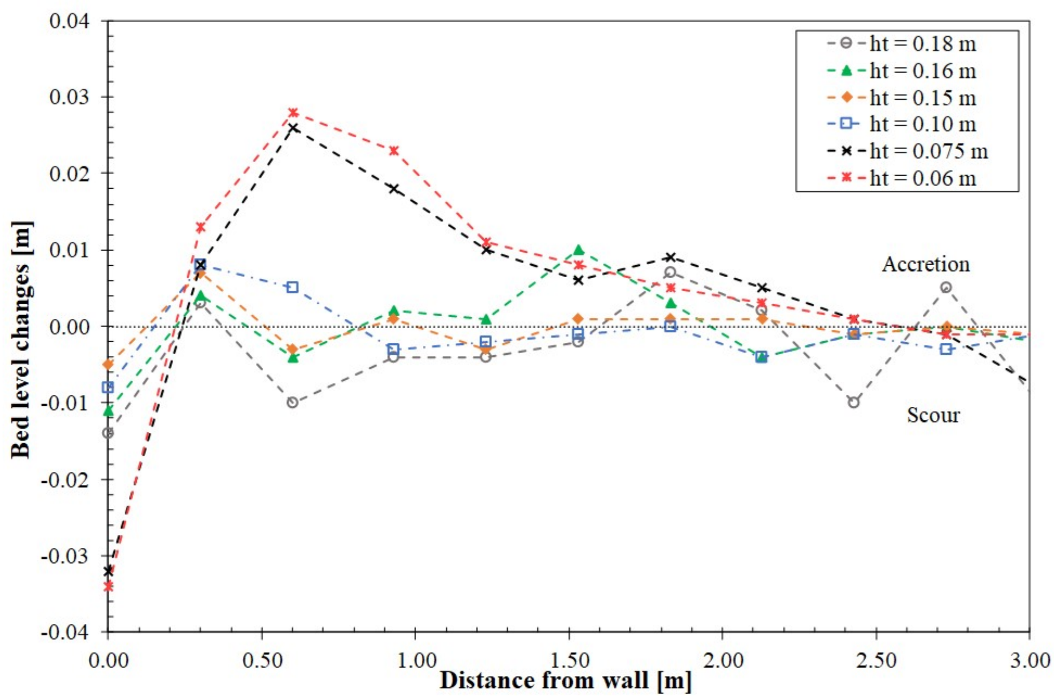

Fig. 10. Bed level changes after 1000 waves - a) s_{op} = 0.02, H_{m0} = 0.085 m b) s_{op} = 0.05, H_{m0} = 0.12 m

Relationship between scour depth and relative water depth

The non-dimensional toe scour depth ($S_t / H_{1/3}$) at a plain vertical wall on shingle beds as a function of relative toe water depth is presented in Fig. 11. Negative values of non-dimensional toe scour depth represent the accretion at the structure.

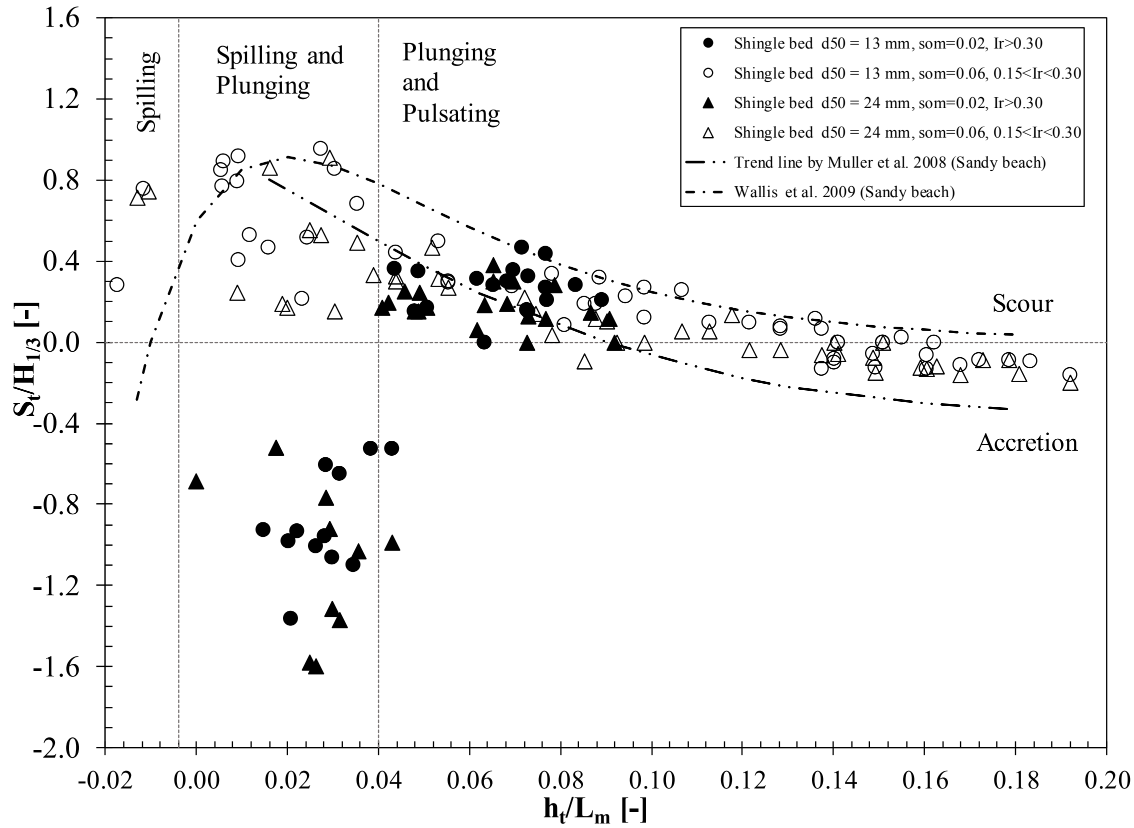

Fig. 11. Variation of non-dimensional toe scour depth at a plain vertical wall with relative toe water depth

Based on experimental and field studies, Sutherland et al. (2006) and Müller et al. (2008) concluded that maximum toe scour depths at a plain vertical seawall on a sandy bed occurs under plunging wave impacts. Similar trends of the maximum toe scour depths were also observed within this study, as shown in Fig. 11. Within experimental limitations, the results show that the greatest toe scour depth (accretion or scouring) occurs for the spilling and plunging waves ($0.005 \leq h_t/L_m$

≤ 0.04). For example, maximum accretion is observed around $S_t/H_{1/3}$ =1.60 and maximum erosion is reported $S_t/H_{1/3}$ = 0.95 at relative toe water depth (h_t/L_m) of about 0.025 under spilling and plunging conditions.

For plunging and pulsating breakers (h_t/L_m > 0.04), the data points demonstrate that the overall non- dimensional toe scour depth continued to decrease, as the relative toe water depth increased. For relatively high-water depths (h_t/L_m > 0.10), the results show accretion at the toe of the vertical wall on a shingle beach with similar features reported by Müller et al. (2008); Wallis et al. (2009) for a sandy beach. In general, the results demonstrate that the accretion at the toe of the structure occurred for waves with low wave steepness (long period), whereas scouring at the structure was observed for high wave steepness, subjected to spilling and plunging conditions.

Relationship between scour depth and Iribarren number

The Iribarren number (Ir) or surf similarity parameter is the combination of structure slope and wave steepness (see Equation 14), which describes wave breaking types.

$$I_r = \frac{tan\propto}{\sqrt{\frac{H_{m0}}{L_{m-1,0}}}} \qquad (14)$$

Where, α is the slope of the structure, H_{m0} is the spectral significant wave height and $L_{m-1,0}$ is the deep water wave length.

For the conditions tested within this study, the Iribarren number, I_r was varied from 0.15 to 0.40 and categorised into two ranges as following:

- $0.15 < I_r < 0.30$ and
- $Ir > 0.30$

The data points in Fig. 11 show that for a certain relative toe water depth, the maximum toe scour depths occur for the larger Iribarren numbers. Similar characteristics were reported by Müller et al. (2008); Wallis et al. (2009) on sandy beaches.

5. Implications for Design

The preliminary design guidance for the estimation of mean overtopping discharges at a plain vertical wall under both impulsive and non-impulsive conditions presented in this paper is an extension to those reported in EurOtop (2016). The new overtopping manual EurOtop (2016) suggested Equation 1 for non-impulsive and Equation 2- 3 for impulsive wave conditions to predict average overtopping rate at vertical structures. Within experimental limitations, the results of this study demonstrate that for both impulsive and non-impulsive wave conditions the mean overtopping is reduced noticeably with the use of shingle beaches, when compared to an impermeable beach profile. For a permeable shingle 1:20 foreshore slope, the alternative formulae (Equation 10-13) can be applied to predict mean overtopping rate at a plain vertical wall under both impulsive and non-impulsive wave conditions. In the absence of any other information to the contrary, a conservative approach is recommended, i.e. an impermeable beach configuration, see prediction formulae (Equation 1-3) reported by EurOtop (2016).

Overall, the probability of overtopping waves at a plain vertical wall on shingle beds were slightly lower than the impermeable bed configuration. However, as observed in Fig 6c. and Fig. 7, it is noticeable from the present research that the maximum individual overtopping wave volumes measured for shingle foreshores do not differ from those measured for impermeable slopes. Due to stochastic nature of wave by wave overtopping, a conservative approach is recommended to estimate the maximum individual overtopping volumes and proportion of overtopping waves, i.e. empirical predictions reported by EurOtop (2016) considering an impermeable beach profile.

Currently, there is no known design guidance to estimate the mean overtopping sediment rates at a plain vertical seawall, the initial step is to establish whether the waves at the toe of the seawall are likely to be broken wave conditions. For non-impulsive and impulsive waves with conditions in the range, $(h_t^2/(H_{m0}L_{m-1,0}) > 0.03)$, sediment within in the overtopping waves are less likely. Under impulsive conditions, in the range of $h_t^2/(H_{m0}L_{m-1,0}) < 0.03$, it is expected to have up to 0.5% of sediment within the overtopping waves.

6. Discussions

The purpose of this small-scale laboratory study was to investigate the wave overtopping and scouring at a plain vertical wall on permeable shingle foreshores and to develop the design guidance that can be applied to predict processes at full-scale. It is however apparent that the outputs of small scale model tests could be perverted by scale and model effects.

In 2002, Pearson et. al. concluded that for battered seawalls (near vertical walls) scale and model effects in small scale physical tests are not significant when compared with large scale laboratory experiments for the estimation of mean and wave by wave overtopping volumes.

In order to keep the scale effects minimal, the laboratory test set up replicated the guidelines of typical small-scale investigations by EurOtop (2016), Powell (1990) and Wolters et al. (2009). To minimize model effects by mitigating reflection from model boundaries, an active wave reflection system was applied. Also, experiments were executed without the presence of the structure to calibrate the incident wave conditions. It is therefore believed that the design guidance of this small scale physical study can be applied at prototype situations without having any significant scale and model effects, although further validation would clearly be desirable.

7. Conclusions

In this study, detailed measurements have been undertaken to parameterize the mean overtopping rate, mean sediment rate, individual overtopping volume, probability of overtopping and, scour depths on a plain vertical seawall, for both impermeable and mobile shingle beach configurations. Based on the test results of this study, the following conclusions can be drawn:

Wave Overtopping

- ✓ Within experimental limitations, the resulting overtopping characteristics correspond to solid impermeable bed showed an overall good agreement with the predictive method of EurOtop (2016) under both impulsive and non-impulsive wave conditions.
- ✓ For impulsive wave conditions tested within this study, it was observed that the mean overtopping rate is reduced by factor 3 and 4 for d_{50} of 13 mm and 24 mm respectively, when impermeable and shingle beaches are compared. For non-impulsive waves, the reduction factors were 1.5 for d_{50} of 13 mm and 2 for d_{50} of 24 mm.
- ✓ For non-impulsive and impulsive waves with conditions in the range, $(h_t^2/(H_{m0}L_{m-1,0}) > 0.03)$, no sediment was reported to pass the crest of the structure. Under impulsive conditions, in the range of $h_t^2/(H_{m0}L_{m-1,0}) < 0.03$, the measured volume of sediment passing the crest of the seawall was around 0.5% of the total volume of the overtopped water.
- ✓ In general, the maximum individual overtopping wave volumes measured for shingle foreshores did not differ from those measured for impermeable slopes.

- ✓ The measured probability of overtopping waves at a plain vertical wall on a shingle bed were slightly lower than the impermeable bed configuration.

Toe scouring

- ✓ For the tested conditions, it was observed that the relative toe scour depth at a plain vertical wall on a shingle beach, is influenced by the relative toe water depth and Iribarren number. For relative toe water depths in the range $0.016 \leq h_t/L_m \leq 0.18$, similar characteristics were reported by Sutherland et al. (2006) on sandy beaches.
- ✓ Maximum scour depths occurred for spilling and plunging waves ($0.005 \leq h_t/L_m \leq 0.04$). Peak accretion was observed $S_t/H_{1/3}$ =1.60 and peak erosion was reported $S_t/H_{1/3}$ =0.95 at relative toe water depths (h_t/L_m), around 0.025.

Prior to this study, limited design guidance was available to predict the mean overtopping discharges and mean sediment rates at vertical seawalls on permeable shingle foreshores. Therefore, a new set of prediction formulae (adapted from EurOtop, 2016) are proposed in this study, based on the new laboratory test results, and a comparison with the available prediction methods in literature for vertical walls on impermeable foreshores subjected to both impulsive and non-impulsive wave conditions.

Acknowledgements

The research is supported by a PhD fund of University of Warwick Graduate School under the Chancellor's International Scholarship scheme. The financial support by the Royal Academy of Engineering under the RAEng/The Leverhulme Trust Senior Research Fellowships scheme (2016/2017) – Grant Ref.: LTSRF1516\12\92, is gratefully acknowledged. The authors would also like to thank the anonymous reviewers for their constructive comments and suggestions in the preparation of this manuscript.

Notation

Symbol	Meaning	Unit
a	Scale parameter in Weibull distribution	[-]
b	Shape parameter in Weibull distribution	[-]
d_{50}	Mean sediment size	[mm]
g	Gravitational acceleration	[m/s^2]
h_b	Water depth at breaking	[m]
h_t	Water depth at toe of the structure	[m]
H_{m0}	Significant wave height determined from spectra analysis	[m]
H_s	Significant wave height determined from time series analysis (=$H_{1/3}$)	[m]
I_r	Iribarren number or breaker parameter	[-]
L_m	Mean wave length based on linear theory ($gT_m^2/2\pi$)	[m]
$L_{m-1,0}$	Spectral wave length based on linear theory ($gT_{m-1,0}^2/2\pi$)	[m]
N_{ow}	Number of overtopping waves	[-]
N_w	Number of incident waves	[-]
P_{ow}	Probability of overtopping per wave (N_{ow}/N_w)	[-]
P(V)	Probability of exceedance of overtopping volume	[-]
q	Mean overtopping discharge per m width	[m^3/s per m]
R_c	Crest freeboard	[m]
s_{max}	Maximum scour depth	[m]
s_t	Toe scour depth	[m]
s_{tmax}	Maximum toe scour depth	[m]
s_m	Wave steepness based on average wave period ($2\pi H_{m0}/gT_m^2$)	[-]
$s_{m-1,0}$	Wave steepness based on mean spectral period ($2\pi H_{m0}/gT_{m-1,0}^2$)	[-]
s_{op}	Wave steepness for spectral peak period ($2\pi H_{m0}/gT_p^2$)	[-]
T_m	Average wave period calculated from time series analysis	[s]
$T_{m-1,0}$	Average spectral wave period defined from spectral analysis by m_{-1}/m_0	[s]
T_p	Spectral peak wave period	[s]
V	Volume of overtopping wave per m width	[m^3 per m]
V_{bar}	Mean overtopping volume per m width	[m^3 per m]
V_{max}	Maximum individual overtopping volume per m width	[m^3 per m]
α	Slope of the structure	[radians]
γ	Peak enhancement factor of JONSWAP energy spectrum	[-]
Γ	Mathematical gamma function	[-]

References

Altomare, C., Gentile, G.M., 2011. Monitoring phases of the re-naturalization process of the Torre del Porto beach. In: Proceedings of the 5th International Short Conference on Applied Coastal Research, RWTH Aachen University, Germany, pp. 414-421.

Altomare, C., Gentile, G.M., 2013. An innovative methodology for the re-naturalization process of a shingle beach. In: Proceedings of the 12th International Coastal Symposium (Plymouth, England), Journal of Coastal Research, Special Issue No. 65, pp. 1456-1460. ISSN 0749-0208.

Besley, P. 1999. Overtopping of seawalls – design and assessment manual. R&D Technical Report W 178, Environment Agency, UK. ISBN 1 85705 069 X.

Bradbury, A., 2000. Predicting breaching of shingle barrier beaches-recent advances to aid beach management. In: Proceedings of the 35th Annual MAFF Conference on River and Coastal Engineering, pp. 05.3.1-05.3.13.

Bruce, T., Van Der Meer, J. W., Pullen, T. & Allsop, N. W. H., 2010. Wave Overtopping at Vertical and Steep Structures. In: Kim, Y. C. (ed.) Chapter 16 in Handbook of Coastal and Ocean Engineering. World Scientific.

Dean, R. G., 1973. Heuristic Models of Sand Transport in the Surf Zone. In: Proceedings of the Conference on Engineering Dynamics in the Surf Zone, Institution of Civil Engineers, Australia, Sydney, pp. 208-214.

De San Román-Blanco, B. L., Coates, T. T., Holmes, P., Chadwick, A. J., Bradbury, A., Baldock, T. E., Pedrozo-Acuna, A., Lawrence, J., Grüne, J., 2006. Large scale experiments on gravel and mixed beaches: Experimental procedure, data documentation and initial results. Coastal Engineering 53(4), 349-362.

Eurotop, 2007. Wave Overtopping of Sea Defences and Related Structures: Assessment Manual. Expertise Netwerk- UK: N. W. H. Allsop, T. Pullen, T. Bruce. NL: J. W. Van der Meer. DE: H. Schüttrumpf, A. Kortenhaus.

Eurotop, 2016. EurOtop II - Manual on wave overtopping of sea defences and related structures: An overtopping manual largely based on European research, but for worldwide application. (Available to download from www.overtopping-manual.com, in press).

Fowler, J. E., 1992. Scour problems and methods for prediction of maximum scour at vertical seawalls. In: Us Army Corps of Engineers, W. E. S. (eds.), Technical Report CERC-92-16, Coastal Engineering Research Center, Vicksburg, MS, USA.

Gentile, G.M., Giasi, C., 2003. An example of eco-compatible methodology for coastal remodelling. In: Proceedings of the European Conference on Application of Methodology, Roma.

Holthuijsen, L. H., 2007. Waves in oceanic and coastal waters. Cambridge University Press, Cambridge.

Jayaratne, R., Mendoza, E., Silva, R., Gutiérrez, F., 2015. Laboratory Modelling of Scour on Seawalls. Presented in the International Conference on Coastal Structures, ASCE, Boston, MA, USA.

Jayaratne, R., Premaratne, B., Adewale, A., Mikami, T., Matsuba, S., Shibayama, T., Esteban, M., Nistor, I., 2016. Failure Mechanisms and Local Scour at Coastal Structures Induced by Tsunami. Coastal Engineering Journal 58(4),1640017.

Klopman, G. and Van der Meer, J.W., 1999.Random wave measurements in front of reflective structures. Journal of Waterway Port Coast and Ocean Engineering 125 (1), pp. 39-45.

Komer, P. D. and Miller, M. C., 1973. The threshold of sediment movement under oscillatory water waves. Journal of Sedimentary Petrology 43(4), pp. 1101-1110.

Kraus, N. C. & Smith, J. M., 1994. SUPERTANK laboratory data collection project. Volume 1: Main Text. Technical Report CERC-94-3, US Army Corps of Engineers Waterways Experiment Station, Coastal Engineering Research Center, Vicksburg. MS, USA, pp. 2191-2204.

Lorang, M. S., 2002. Predicting the crest height of a gravel beach. Geomorphology, 48(1), 87-101.

Mansard, E.P.D., Funke, E.R., 1980. The measurement of incident and reflected spectra using a least squares method. Coastal Engineering 154–172.

Matias, A., Williams, J. J., Masselink, G., Ferreira, Ó., 2012. Overwash threshold for gravel barriers. Coastal Engineering 63, 48-61.

McCall, R., Masselink, G., Poate, T., Roelvink, J., Almeida, L., 2015. Modelling the morphodynamics of gravel beaches during storms with XBeach-G. Coastal Engineering 103, 52-66.

Müller, G., Allsop, W., Bruce, T., Kortenhaus, A., Pearce, A., Sutherland, J., 2008. The occurrence and effects of wave impacts. In: Proceedings of the ICE-Maritime Engineering (ICE), pp. 167-173.

Obhrai, C., Powell, K., Bradbury, A., 2008., A laboratory study of overtopping and breaching of shingle barrier beaches. In: Proceedings of the Coastal Engineering Conference, ASCE, Hannover, Germany, pp. 1497-1508.

Owen, M. W., (1980). Design of sea walls allowing for wave overtopping. Report EX 924, Hydraulics Research Station, Wallingford, UK.

Pearce, A., Sutherland, J., Müller, G., Rycroft, D., Whitehouse, R., 2006., Scour at a seawall-field measurements and physical modelling. In: Proceedings of the 30th International Conference on Coastal Engineering, ASCE, San Diego, USA.

Pearson, J. M., Bruce, T., Allsop, N. W. H., Gironella, X., 2002. Violent wave overtopping-measurements at large and small scale. In: Proceedings of the 28th International Coastal Engineering Conference, ASCE, Cardiff, UK, pp. 2227-2238.

Pearson, J. M., 2010. Overtopping and Toe Scour at Vertical Seawalls. In: Proceedings of the 9th international conference on Coasts, marine structures and breakwaters: Adapting to change, Institution of Civil Engineers, Thomas Telford Ltd, Edinburgh, pp. 598-608.

Pourzangbar, A., Saber, A., Yeganeh-Bakhtiary, A., Ahari, L. R., 2017. Predicting scour depth at seawalls using GP and ANNs. Journal of Hydroinformatics, jh2017125.

Powell, K. A., 1990. Predicting short term profile response for shingle beaches. Report SR 219, HR Wallingford,Wallingford, UK.

Powell, K. A., Lowe, J. P., 1994. The scouring of sediments at the toe of seawalls. In: Proceedings of the Hornafjordor International Coastal Symposium, Iceland, pp. 749-755.

Sutherland, J., Brampton, A. H., Motyka, G., Blanco, B., Whitehouse, R. J. W. 2003. Beach lowering in front of coastal structures-Research Scoping Study. Report FD1916/TR, London, UK. INTERNET: available from http://sciencesearch. defra. gov. uk/(page accessed 14/02/17).

Sutherland, J., Obhrai, C., Whitehouse, R., Pearce, A., 2006. Laboratory tests of scour at a seawall. In: Proceedings of the 3rd International Conference on Scour and Erosion, CURNET, Technical University of Denmark, Gouda, The Netherlands.

Sutherland, J., Brampton, A. H., Obrai, C., Dunn, S., Whitehouse, R. J. W., 2008. Understanding the lowering of beaches in front of coastal defence structures, Stage 2-Research Scoping Study. Report FD1927/TR, London, UK. INTERNET: available from http://sciencesearch. defra. gov. uk/(page accessed 20/02/17).

Tahersima, M., Yeganeh-Bakhtiary, A., Hajivalie, F., 2011. Scour pattern in front of vertical breakwater with wave overtopping. Journal of Coastal Research 64, 598.

Tofany, N., Ahmad, M., Kartono, A., Mamat, M., Mohd-Lokman, H., 2014. Numerical modeling of the hydrodynamics of standing wave and scouring in front of impermeable breakwaters with different steepnesses. Ocean Engineering 88, 255-270.

Tsai, C. P., Chen, H. B., You, S. S., 2009. Toe scour of seawall on a steep seabed by breaking waves. Journal of waterway, port, coastal, and ocean Engineering 135(2), 61-68.

Van Der Meer, J. W., 1992. Stability of the seaward slope of berm breakwaters. Coastal Engineering 16(2), 205-234.

Van der Meer, J.W., Janssen, J. P. F. M., 1994. Wave run-up and wave overtopping at dikes. In: Wave forces on inclined and vertical wall structures, ed. N. Kobayashi and Z. Demirbilek, ASCE, pp. 1-27.

Van Hijum, E., Pilarczyk, K., 1982. Equilibrium profile and longshore transport of coarse material under regular and irregular wave attack. Publication No. 174, Delft Hydraulics laboratory, Delft, Netherlands.

Victor, L., Van der Meer, J. W., Troch, P., 2012. Probability distribution of individual wave overtopping volumes for smooth impermeable steep slopes with low crest freeboards. Coastal Engineering 64, 87-101.

Wallis, M., Whitehouse, R. & Lyness, N., 2009. Development of guidance for the management of the toe of coastal defence structures. Presented in the 44th Defra Flood and Coastal Management Conference, Telford, UK.

Williams, J. J., Buscombe, D., Masselink, G., Turner, I., Swinkels, C., 2012a. Barrier Dynamics Experiment (BARDEX): aims, design and procedures. Coastal Engineering 63, 3-12.

Williams, J. J., De Alegría-Arzaburu, A. R., McCall, R. T., Van Dongeren, A., 2012b. Modelling gravel barrier profile response to combined waves and tides using XBeach: Laboratory and field results. Coastal Engineering 63, 62-80.

Wolters, G., Van Gent, M., Allsop, N. W. H., Hamm, L., Mühlestein, D., 2009. HYDRALAB III: Guidelines for physical model testing of rubble mound breakwaters. In: Proceedings of the 9th International Conference on Coasts, Marine Structures and Breakwaters: Adapting to Change, Edinburgh, United Kingdom, pp. 659-670.

Xie, S. L., 1981. Scouring patterns in front of vertical breakwaters and their influences on the stability of the foundation of the breakwaters. Department of Civil Engineering, Delft University of Technology, Delft, The Netherlands.

Yalin, S., 1963. A model shingle beach with permeability and drag forces reproduced. In: Proceedings of the 10th IAHR Congress 1963. London pp.169.

Zanuttigh, B., Van Der Meer, J. W., Bruce, T., Hughes, S., 2013. Statistical characterisation of extreme overtopping wave volumes. In: Proceedings of ICE, Coasts, Marine Structures and Breakwaters, Edinburgh, UK.